Semi-annual report for NASA Grant NAG5-1125 entitled

"The Role of Global Cloud Climatologies in Validating Numerical Models"

Principal Investigator: Harshvardhan
Department of Earth and Atmospheric Sciences
Purdue University
West Lafayette, Indiana 47907

April 1, 1991 - September 30, 1991

The grant period covered in this report was devoted to preparing for publication and presentation our work on longwave surface radiation. The net upward longwave surface radiation is exceedingly difficult to measure from space. A hybrid method using GCM simulations and satellite data from ERBE and ISCCP has been utilized to produce global maps of this quantity over oceanic areas.

This work will be presented at the ECMWF/GEWEX Workshop on The Hydrology and Surface Radiation in Atmospheric Models to be held in Reading, U.K., 28 October - 1 November, 1991. A manuscript that we have prepared for this workshop showing all the results is attached as the Semi-Annual Progress Report.

THE USE OF TOA CLOUD LONGWAVE RADIATIVE FORCING TO ESTIMATE MEAN MONTHLY SURFACE LONGWAVE RADIATION

Harshvardhan
Department of Earth and Atmospheric Sciences
Purdue University
West Lafayette, IN 47907

1. Introduction

The surface radiation budget, i.e., the net solar radiation absorbed minus the net longwave radiation emitted, and its spatial and temporal variations are key parameters in climate and weather studies. This budget plays a major role in determining radiative heating, as well as sensible and latent heat fluxes over ocean and land surfaces. As a result, the net radiative flux constitutes an important boundary forcing for the general ocean circulation and a crucial parameter for determining meridional oceanic heat transport, ocean-atmosphere interaction and land-atmosphere interaction. Moreover, it is a useful parameter when addressing issues related to climate change due to CO_2 and other trace gases, and in the validation of radiation schemes used in climate models. Therefore, it is understandable for the atmospheric and oceanic communities to need reliable estimates of the surface radiation budget (WCP-92 1984).

Direct high-quality radiation measurements at the surface are difficult to make, particularly over the oceans which cover more than 60% of the Earth's surface. Actually there are very few surface stations measuring the radiation budget routinely and reliably because of the requirement of careful instrument calibration and temperature correction for the radiation, especially longwave, measurement. In addition, because of operating costs, it is not feasible to maintain a network of surface stations over the oceans. Although an attempt has been made to use ships to observe some meteorological parameters such as sea surface temperature, air temperature, specific humidity near the surface and even fractional cloud coverage, there has not been much progress in the measurement of surface radiation. Few ships measure radiation quantities because of problems with instrument calibration. Moreover, regular ship observations are limited along commercial shipping lanes, and vast geographic gaps still exist, especially in the southern hemisphere. Consequently, the empirical formulas used to derive budgets have been validated only over limited regions, and when applied globally, large errors are inevitable. Therefore, direct measurement of shortwave and longwave radiation fluxes at the surface globally has not been possible.

Since there are difficulties in obtaining radiative data from surface stations routinely and reliably, it has been realized that space based observations are the only means to have global coverage. However, because of the intervening atmosphere, the surface radiation budget is difficult to measure from satellites, whereas the top-of-the-atmosphere (TOA) radiation balance can be measured directly. Over the past decades, considerable effort has been expended in the global measurement of the TOA radiation budget. Attempts at inferring the surface radiation budget from space based measurements have only begun recently.

There has been some success in obtaining the solar radiation budget at the surface (e.g. Raschke and Preuss 1979; Tarpley 1979; Gautier et al. 1980; Pinker and Ewing 1985; Justus et al. 1986). The progress in surface longwave radiation budget measurements by satellite, however, has been much slower. Currently, some techniques are available to estimate the downward longwave component of the surface flux (Darnell et al. 1983, 1986; Chou 1985; Schmetz et al. 1986; Frouin et al. 1988; Ardanuy et al. 1989; Wu and Cheng 1989; Breon et al. 1991). The net longwave component at the surface can be estimated by the difference between the upwelling and downwelling fluxes. The upward component is determined directly from sea surface temperature since the oceanic surface emits essentially as a blackbody. The downward flux, however, is more difficult to obtain since it depends on many

meteorological parameters such as atmospheric moisture, temperature and cloud cover. Because of the uncertainty of the measurement of these meteorological parameters, at present there is a need for improvement in the estimation of net longwave radiation fluxes at the surface.

Two types of methods have been used to estimate the downward longwave flux at the surface: statistical and physical. As the name implies, statistical methods rely on correlation between fluxes and observed meteorological parameters. The physical techniques are based on modeling radiative processes occurring in the atmosphere (clear and cloudy atmosphere). The downward flux is computed from radiative transfer models which utilize parameters obtained from satellite radiance data. These parameters include temperature and water vapor mixing ratio profiles, fraction of cloud coverage and cloud emittance. However, all physical methods currently under consideration have to make certain assumptions regarding both the presence of clouds and their vertical extent. Recent examples of these attempts are Chou (1985), Schmetz et al. (1986), Darnell et al. (1986), Gupta (1988), and Wu and Cheng (1989). The treatment of longwave radiation transmittance in the presence of clouds becomes more complex since knowledge of cloud top and base heights and emittances are required. For this reason, it is important to determine the vertical profile of cloudiness as well as the horizontal distribution of clouds and associated emittances. Unfortunately, determination of the vertical profile of cloudiness from space based measurements is difficult since overlap of cloudy layers is common in the real atmosphere. Therefore, because of the uncertainties in assumed cloudiness, all these methods often give unreliable results.

The method used here to obtain monthly mean quantities avoids the explicit computation of cloud fraction and the location of cloud base in estimating the downward longwave radiation globally (Harshvardhan et al. 1990). An advantage of this technique is that no independent knowledge or assumptions regarding cloud cover for a particular month are required. The only information required is a relationship between the cloud radiative forcing (CRF) at the top of the atmosphere and that at the surface, which is obtained from a general circulation model (GCM) simulation.

2.   Method

The cloud radiative forcing (CRF) has been defined as the difference between the radiative flux as measured or computed and the clear sky flux (Charlock and Ramanathan 1985; Ramanathan 1987). For example, the longwave cloud radiative forcing at the surface is

$$\text{Surface LWCRF} = \text{Surface LW Flux} - \text{Clear Sky Surface LW Flux.} \tag{1}$$

Previous studies have shown that there is no correlation between the spectrally integrated outgoing longwave radiation and the net longwave at the surface (Ramanathan 1986; Weare 1989). But Harshvardhan et al. (1990) have recently come to the conclusion that there is a relationship between the longwave CRF at the top of the atmosphere and the surface in model simulations. This relationship has been explained on the grounds that clouds of a certain type tend to form preferentially over certain geographic areas. The technique proposed by Harshvardhan et al. (1990) to estimate surface longwave fluxes starts with the GCM simulated climatological ratio of the CRF at the top and at the surface along with the longwave CRF at the top of the atmosphere obtained from the Earth Radiation Budget Experiment (ERBE; Ramanathan 1987) to compute the surface longwave CRF for the particular month. In this way, no independent knowledge or assumptions about cloud

cover are involved, thus avoiding the most uncertain step in other methods of estimating the longwave radiation budget at the surface. The next step in the procedure is to obtain an estimate of the clear sky downward longwave flux and upward emission at the surface.

As mentioned before, the downwelling longwave radiation at the surface can not be measured directly from space, but profiles of temperature and water vapor mixing ratio in clear columns are routinely obtained from inversions of measured radiances. Most attempts to compute the downwelling longwave fluxes have relied on these retrieved profiles to furnish the flux using a radiative transfer model.

Here we show results using the once daily profile contained in the data released by the International Satellite Cloud Climatology Project (ISCCP; Schiffer and Rossow 1983). ISCCP C1 data provides a daily profile of temperature and precipitable water as well as surface temperature at a 2.5° x 2.5° horizontal resolution. This information from TOVS (Tiros Operational Vertical Sounder) is used to generate clear sky downward longwave fluxes globally and upward fluxes only over the ocean where the once-a-day sampling is acceptable. The diurnal cycle of surface temperature precludes using this technique over land. The radiation code used to compute the clear sky downward flux is the one used in the UCLA/GLA (now CSU) GCM (Harshvardhan et al. 1989).

A flow diagram of the technique used to obtain surface longwave fluxes is shown in Fig. 1. Calculations start from the relationship between the longwave CRF at the top of the atmosphere and at the surface (Harshvardhan et al. 1990). Results for the months of January, April, July and October are used in this study and represent the simulated monthly characteristics of this relation over the annual cycle. The longwave CRF at the top of the atmosphere as obtained from ERBE is combined with the relationship to obtain the longwave CRF at the surface for each of the four months. Then, by means of the radiative transfer model, with input meteorological parameters such as temperature profile and water vapor mixing ratio profile and sea surface temperature from ISCCP data as well as standard ozone vertical distributions, the clear-sky downward longwave radiative flux and the clear-sky net longwave upward radiation flux at the surface are obtained. Because ozone is primarily confined to the stratosphere, its contribution to downward longwave flux is much less than that of other parameters such as water vapor in the lower atmosphere. Therefore, use of a standard ozone profile is justified.

In general, it is difficult to obtain satellite estimates of clear-sky flux that do not suffer from some cloud contamination due to a combination of subsensor resolution cloud elements and clouds that may not be detectable with the spectral intervals of the current radiometer. In this study, the clear sky fluxes are computed for the atmospheric structure under cloudy conditions, but assuming a cloud-free sky. Since the CRF at the surface and the clear-sky radiative fluxes at the surface are available, based on the definition of the CRF shown in equation (1), the actual radiative fluxes are calculated simply as the clear-sky flux plus the corresponding CRF.

```
    ┌─────────┐              ┌─────────┐                ┌──────────┐
    │   GCM   │              │  ERBE   │                │  ISCCP   │
    └────┬────┘              └────┬────┘                └────┬─────┘
         │                        │                          │
         ▼                        ▼                          ▼
┌──────────────────┐      ┌──────────────┐        ┌──────────────┐
│ Relationship     │      │  CRF at the  │        │  Longwave    │
│ between          │      │  top of the  │        │  radiation   │
│ the LW CRF at    │      │  atmosphere  │        │  model       │
│ the top          │      │              │        │              │
│ of the atmosphere│      └──────┬───────┘        └──────┬───────┘
│ and the surface  │             │                       │
└────────┬─────────┘             │                       │
         │                       │                       │
         ▼                       ▼                       ▼
┌─────────────┐      ┌──────────────────┐      ┌──────────────────┐
│ CRF at the  │      │ Clear-sky        │      │ Clear-sky net    │
│ surface     │      │ downward         │      │ upward           │
│             │      │ longwave         │      │ longwave         │
│             │      │ radiative        │      │ radiative        │
│             │      │ flux at the      │      │ flux at the      │
│             │      │ surface          │      │ surface          │
└──────┬──────┘      └────────┬─────────┘      └────────┬─────────┘
       │                      │                         │
       ▼                      ▼                         ▼
┌──────────────────────┐          ┌──────────────────────┐
│ Downward longwave    │          │ Net upward longwave  │
│ radiative flux at    │          │ radiative flux at    │
│ the surface          │          │ the surface          │
└──────────────────────┘          └──────────────────────┘
```
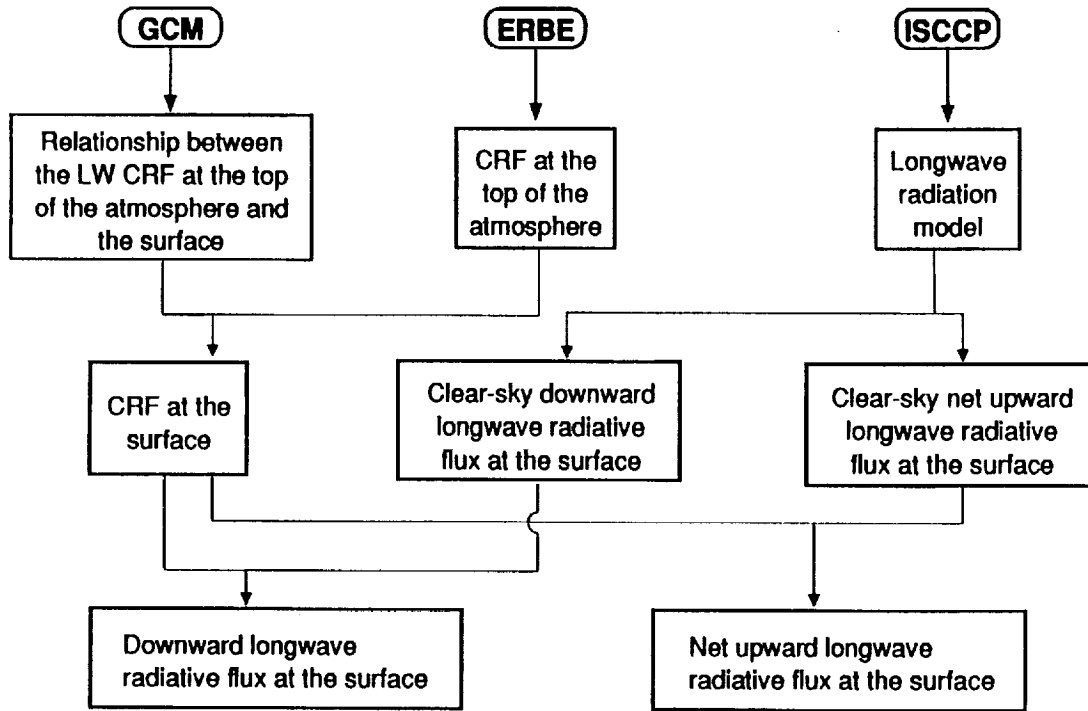
Figure 1.   Flow diagram of the procedure to obtain maps of the monthly mean net upward longwave
             radiation flux at the surface using information provided by a general circulation model
             (GCM), data from the Earth Radiation Budget Experiment (ERBE) and the International
             Satellite Cloud Climatology Project (ISCCP).

3.   Results

a. Longwave CRF at the Surface (global)

The mean monthly distributions of the longwave cloud radiative forcing (CRF) at the surface are
presented in Fig.2 for the months of April, July and October, 1985 and January 1986. They are derived
by combining the longwave CRF at the top of the atmosphere and the ratios of the CRF at the top to
that at the surface. Based on the definition in equation (1), the longwave CRF is the difference between
the mean longwave flux and clear sky longwave flux for the same period. Here the longwave CRFs
at the top of the atmosphere are retrieved from ERBE satellite data according to this definition. In
the original ERBE data, there are a few regions in the tropics where clear sky longwave radiative
fluxes at the top of the atmosphere are unavailable because of the lack of clear sky pixels during the
experiment period. Therefore, an interpolation is performed to make up the missing data using
neighboring points.

There are several noteworthy features of these distributions. First, regions with small surface
longwave CRF are concentrated in the tropical and the subtropical oceanic areas (Fig.2). Surface CRF

is small in the tropics because the boundary layer there is moist and radiatively opaque even for clear skies. In addition, although clouds are both persistent and widespread over this region, extensive coverage of cloud bases are at high altitudes.

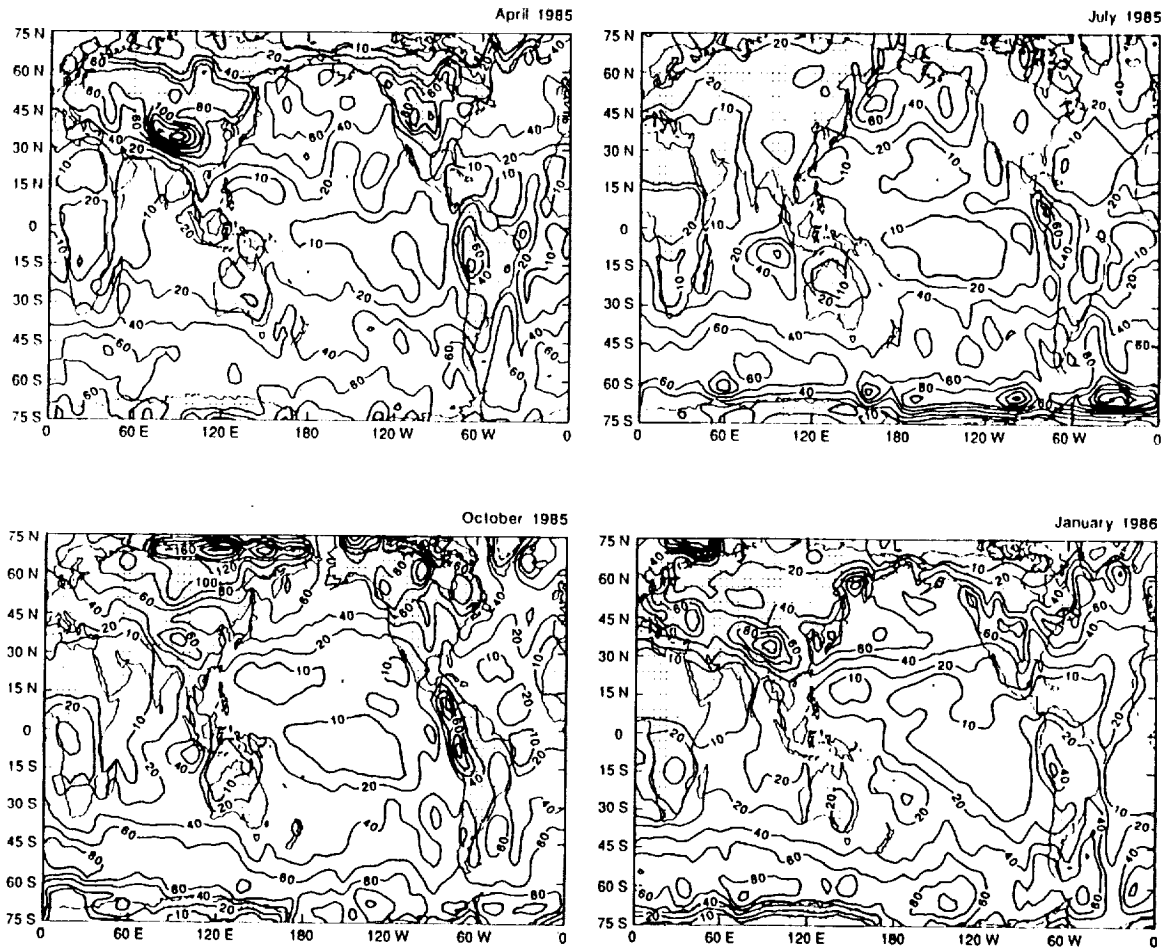Longwave Cloud Radiative Forcing at the Surface

$(W\,m^{-2})$

Figure 2.   Monthly mean longwave cloud radiative forcing at the surface for April, July, October, 1985 and January 1986 obtained from ERBE top-of-the-atmosphere cloud forcing and GCM simulations of cloudiness.

In the central Pacific Ocean, the areas with surface longwave CRF below 20 Wm^{-2} dominate throughout the year. This is also the case for the northern and central Indian Ocean in both April, 1985 and January, 1986. Areas with large surface longwave CRF occur over oceanic areas southwest of Indonesia, with a maximum of more than 60 Wm^{-2} in October and more than 80 Wm^{-2} in July, 1985. Both of these maxima correspond to areas of tropical convective activity. In the central Atlantic Ocean, the surface longwave CRF is below 30 Wm^{-2}.

Much larger values of surface CRFs are found over continents than over oceans during most of the year. The surface values in Eurasia and North American are more than 80 Wm^{-2} in April, 1985 and 60 Wm^{-2} in both October, 1985 and January, 1986. Evidently, all these results correspond to persistent widespread precipitation over the continents. It is interesting to note that small surface CRFs (below 30 Wm^{-2}) emerge over most continents in July, 1985. These low surface CRFs are a consequence of the large CRF ratios over continents computed from the GCM. The model includes the radiative effects of convective anvils but ignores shallow convective clouds. The CRF at the top is therefore quite substantial but the surface CRF is not. Thus the ratio is probably an overestimate. Moreover, there are two continents, Africa and Australia, which always have small surface CRFs throughout the year because of their large desert and semi-arid areas. Fig. 2 shows the surface CRFs there to be often below 30 Wm^{-2}, especially in northern Africa, where the values are always below 20 Wm^{-2}. It is worthwhile noting that a persistent large surface CRF region exists in the tropical region of South America. Obviously, this results from the persistent cloud cover in this region. Over high latitude regions, some areas with the largest surface longwave CRFs are found over the region poleward of 65°S, with a maximum of 150 Wm^{-2} in July and some areas over the Arctic, with a maximum of more than 140 Wm^{-2} in October and January. Two explanations are possible for this phenomenon. Physically, it is reasonable that persistent low clouds over these regions lead to high surface longwave CRF. On the other hand, an underestimate of high cloud over the polar regions in the GCM simulation can also result in the surface longwave CRFs being somewhat unreasonably high. The latter is probably the reason for large longwave CRFs over high latitudes in Fig.2. Finally, areas with the average range of 30-50 Wm^{-2} dominate most mid-latitude oceanic regions of both hemispheres. This is attributable to the increase in oceanic stratus in these regions.

b. *Downward Longwave Radiation Flux at the Surface (global)*

Downward longwave radiative fluxes at the surface for cloud-free skies, as calculated by the radiation code in the UCLA/GLA GCM in conjunction with the input meteorological parameters from the ISCCP satellite data and U. S. standard atmosphere (COESA 1976), are presented in Fig.3 for April, July and October, 1985 and January, 1986 respectively.

Over the oceanic areas, clear sky surface downward longwave fluxes have pronounced zonal distributions, especially in mid-latitudes and near polar regions. In the tropical and subtropical areas, the regions with large downward fluxes (larger than 400 Wm-2) are centered over Southeast Asia in April and October, 1985 and shift a little northward in July, 1985 and, as expected, a little southward in January, 1986. Apparently, over the oceanic areas, the surface downward longwave fluxes of clear skies are related closely with seasonal incident solar energy throughout the year. In the northern spring (April) and fall (October), for the quite symmetrical solar insolation distribution at that time, surface downward longwave fluxes also have a symmetrical distribution with respect

Clear Sky Downward Longwave Flux at the Surface
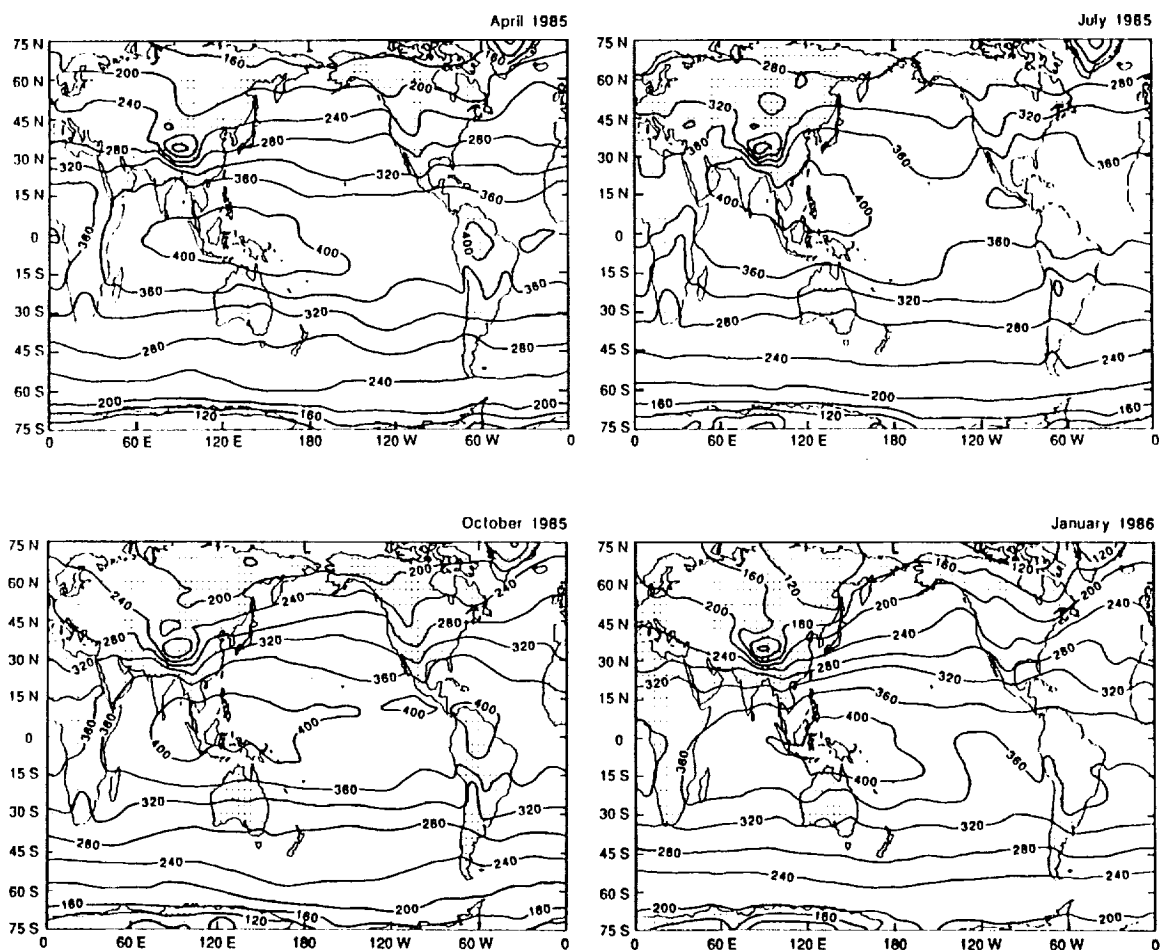$$(W\ m^{-2})$$

Figure 3.   Monthly mean clear sky downward longwave radiation flux at the surface for April, July, October 1985 and January 1986 obtained from TOVS profiles on the ISCCP C1 tapes and a broad band radiation code.

to the equator. In the northern summer (July) and winter (January), the maps of clear sky surface downward fluxes show a shift northward and southward respectively with the zenithal marching of the sun in the same direction. This result is consistent with the fact that clear sky downward fluxes are determined by the near surface temperature which is closely related to the incident solar energy. Evidently, the high values (larger than 400 Wm^{-2}) in Southeast Asia correspond to areas where, due to the high surface temperature of islands, the atmosphere is warmer than elsewhere along the same latitudinal belt. In particular, there is an area with values larger than 420 Wm^{-2} centered east of Papua New Guinea in January, 1986, corresponding to very warm and moist near surface conditions. In

contrast, the low values (less than 200 Wm^{-2}) near the polar regions correspond to areas where the atmosphere is cold and dry throughout the year.

Over the continents, symmetrical distributions of clear sky downward fluxes disappear and more complicated features of distributions emerge, corresponding to the land surface. There is a pronounced center of low values of downward fluxes over the Tibetan Plateau in Asia throughout the year because the mean elevation of the Tibetan Plateau is more than 4000 m above sea level so that surface air temperature is quite low except in summer. However even though high temperatures often occur there in summer, its high elevation makes the air still very dry. Since the major contribution to longwave downward flux at the surface comes from the water vapor in the lower atmosphere, the dry air over that region results in an area of low values of downward fluxes. Over southern Africa, relatively higher values along the same latitude result from the higher air temperature and more moist air. In northern Africa, although the surface temperature is very high, the dry air, due primarily to its desert areas, results in downward fluxes that are lower along the same latitude. In addition, a pronounced trough line along the Rocky Mountains in Fig.3 represents higher altitudes and a drier atmosphere in that region compared to surrounding areas.

Surface downward longwave fluxes, as derived from the formula described in equation (1) with given clear sky fluxes and the longwave CRF at the surface, are presented in Fig.4 for April, July and October, 1985 and January, 1986 respectively. Over the oceanic areas, the zonal distribution for the clear sky case is no longer apparent. The presence of clouds increases the downward fluxes at the surface globally throughout the year. Fluxes with values larger than 400 Wm^{-2} are found over areas associated with the intense convective cloud systems, such as the ITCZ, as well as the summer and winter monsoon areas. It is reasonable because, in these regions, the cloud bases are low and the air temperatures are high. An area with values larger than 440 Wm^{-2} is found over northeast Australia in January, 1986, corresponding to the high temperatures in the austral summer. Also, an area with high values is centered over southwest Indonesia in July, 1985. The map for July, 1985 and January, 1986 compare quite well with the corresponding results of Wu and Cheng (1989) for 1979. Their results were obtained using a physical model based on HIRS 2/MSU retrievals.

Compared with clear sky maps, larger changes occur over land than over the oceans throughout the year. In addition, the regions of high values are still distinguishable in these months except in April, 1985. Low downward fluxes (less than 280 Wm^{-2}) are found over high latitudes and polar regions, where the precipitable water is low and air temperature is cold. As seen in Fig.4, contour lines of downward fluxes are spaced very densely in high latitudes during the whole year. As we mentioned before, these sharp changes perhaps result from uncertainties in modeling the meteorological parameters in these regions. In addition, seasonal variations of surface downward fluxes are still notable in Fig.4, even though they are not as remarkable as in the clear sky case.

c.   *Net Upward longwave Radiation Flux at the Surface (ocean only)*

The clear sky net upward longwave flux at the surface is the difference of the upward flux minus the downward surface flux assuming no clouds. The upward flux here is computed from the sea surface temperature, which is a reported parameter in ISCCP C1   satellite data. There are three surface temperatures (TS) provided by ISCCP: mean TS from a clear sky composite, mean TS for

Atmospheric Downward Longwave Flux at the Surface
$(W\ m^{-2})$

April 1985

July 1985
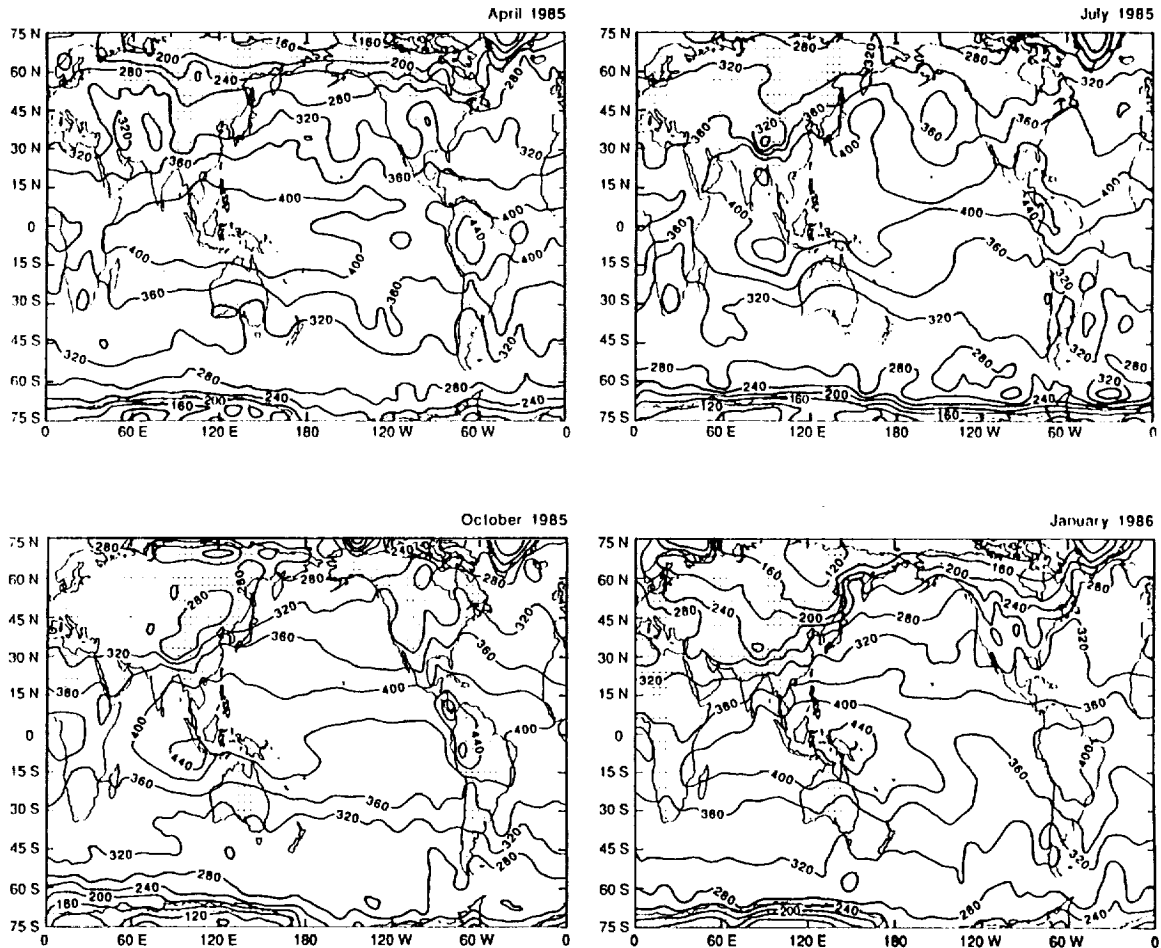
October 1985

January 1986

Figure 4. Monthly mean atmospheric downward longwave radiation flux at the surface for April, July, October 1985 and January 1986 obtained from the clear sky values shown in Figure 3 and the cloud forcing shown in Figure 2.

IR-clear pixels, and mean TS for VIS/IR-clear pixels for only day time. In order to compute the surface emission, it is not necessary to use any of these fields but instead rely on an independent source such as the sea surface temperature provided by NOAA's Climate Analysis Center (CAC). This is a blend of in situ data, advanced very high resolution radiometer (AVHRR) satellite data, and ice data (Reynolds 1988). Fig.5 shows the zonally averaged sea surface temperatures for January, 1986 for the three ISCCP fields and the CAC field. In high latitude regions, the CAC sea surface temperature is much higher than the ISCCP values because ice surface temperature is set to be the freezing point of sea water (-1.8°C). Fig.5 indicates that the clear sky composite TS is warmest among the three ISCCP sea surface temperatures, while the IR clear sky TS is the coldest. This is to be expected since IR clear pixels are contaminated by low level clouds. We chose the VIS/IR clear sky as the most representative quantity for this study.
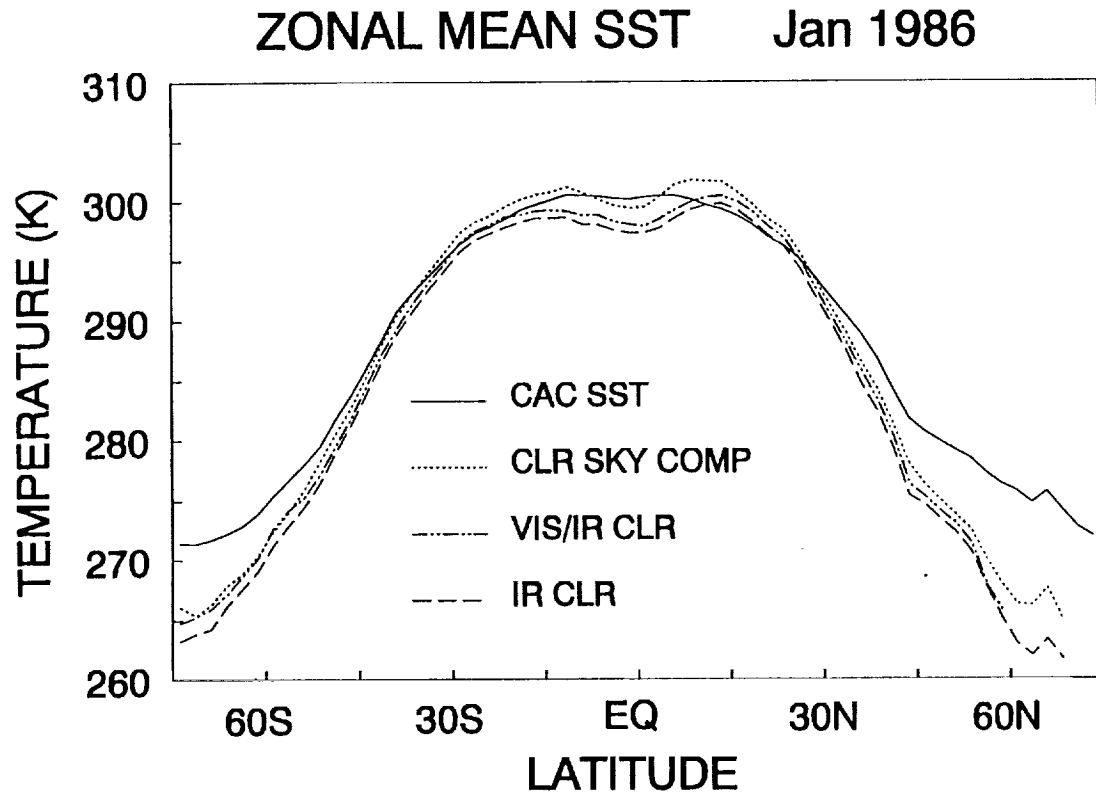
ZONAL MEAN SST   Jan 1986

Figure 5.   Zonal mean sea surface temperatures (SST) for January 1986 from three different parameters on the ISCCP C1 tapes and the blended SST from the Climate Analysis Center (CAC).

The difference between the surface emission computed from daytime mean TS for VIS/IR clear pixels and the CAC sea surface temperature is presented in Fig.6 for January, 1986. This difference is a measure of the uncertainty one may expect in the upward longwave radiation flux computed using different sources for the sea surface temperatures. The dominant feature of this map is a set of biases of less than 10 Wm-2 present over the tropical and subtropical regions except around southeast Asia, where the surface emission from mean TS for VIS/IR clear pixels exceeds that from CAC temperature by as much as 30 Wm^{-2}. The areas with differences larger than 10 Wm^{-2} are found over high latitudes in the Pacific and Atlantic Ocean. Positive differences (less than 10 Wm-2) are located over the central Pacific ocean and eastern Indian ocean, whereas areas with negative difference are found in other locations. The maximum absolute difference is only around 5%. Therefore, the agreement between the two upward fluxes is generally good for this month.

Fig.7 shows the clear sky net upward longwave fluxes at the surface for April, July and October, 1985 and January, 1986 respectively. Physically the maps of clear sky net upward longwave fluxes primarily reflect the distribution of water vapor content in the boundary layer. The area with lowest values is found over Southeastern Asia throughout the year. In this region, even in the absence of clouds, the clear sky net upward longwave fluxes are quite small because of the high water vapor
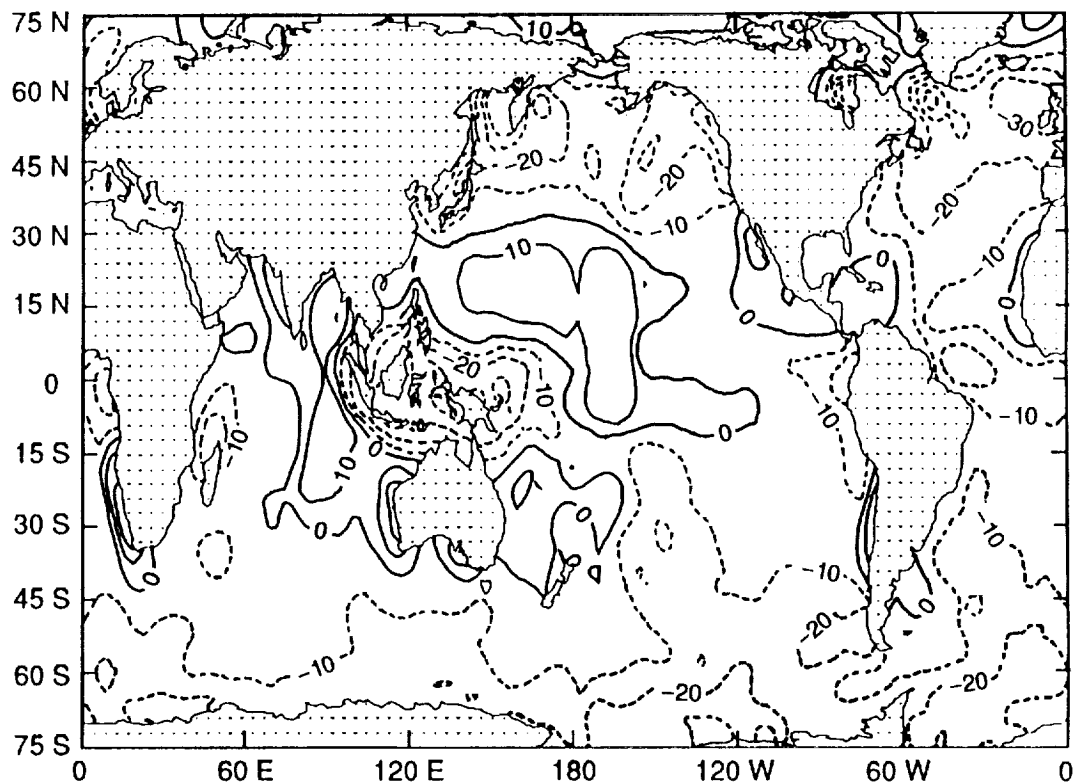
Figure 6.   Difference between the monthly mean surface emission in Wm^{-2} for January 1986 computed using the CAC SST and the VIS/IR clear TS on the ISCCP C1 tapes. A positive difference indicates that the surface emission implied by the CAC SST is higher.

mixing ratio near the surface. Areas with values larger than 100 Wm^{-2} are found over the mid-latitude subsidence zones between 15° and 45° latitude in both hemispheres in April, October, 1985 and January, 1986, and in the southern hemisphere in July, 1985. These are regions in which a dry atmosphere overlies a moderately warm ocean surface. Also, in July, 1985, there is a minimum of less than 40 Wm^{-2} off the coast of central America and, in the other three months, a minimum of less than 40 Wm^{-2} just along the west coast of Colombia, Ecuador and Peru; all these minima correspond to the presence of a relatively moist atmosphere.

Net upward longwave flux, a difference field of the clear sky net upward flux minus the surface longwave CRF (Fig.2) as described in equation (1), is presented in Fig.8 for April, July and October, 1985 and January, 1986. In this case, the areas with smaller values are still found over Southeast Asia. When it is clear, the value is low because the boundary layer is moist; when it is cloudy, there is enhanced downward emission. Also the small net upward fluxes with values less than 40 Wm^{-2} are found in high latitudes and polar regions, where of course, the air temperature is low and thus air is dry throughout the year. Values larger than 80 Wm^{-2} are found over some areas in the tropical and mid-latitude zone. It is worth noting that the negative values near the Antarctic in July, 1985 result from the large longwave CRF at the surface derived previously. Since negative values are possible but unlikely, one may conclude that the unreasonable high surface CRF is a result of the modeling and computation errors but not physical processes. Generally, the influence of clouds in

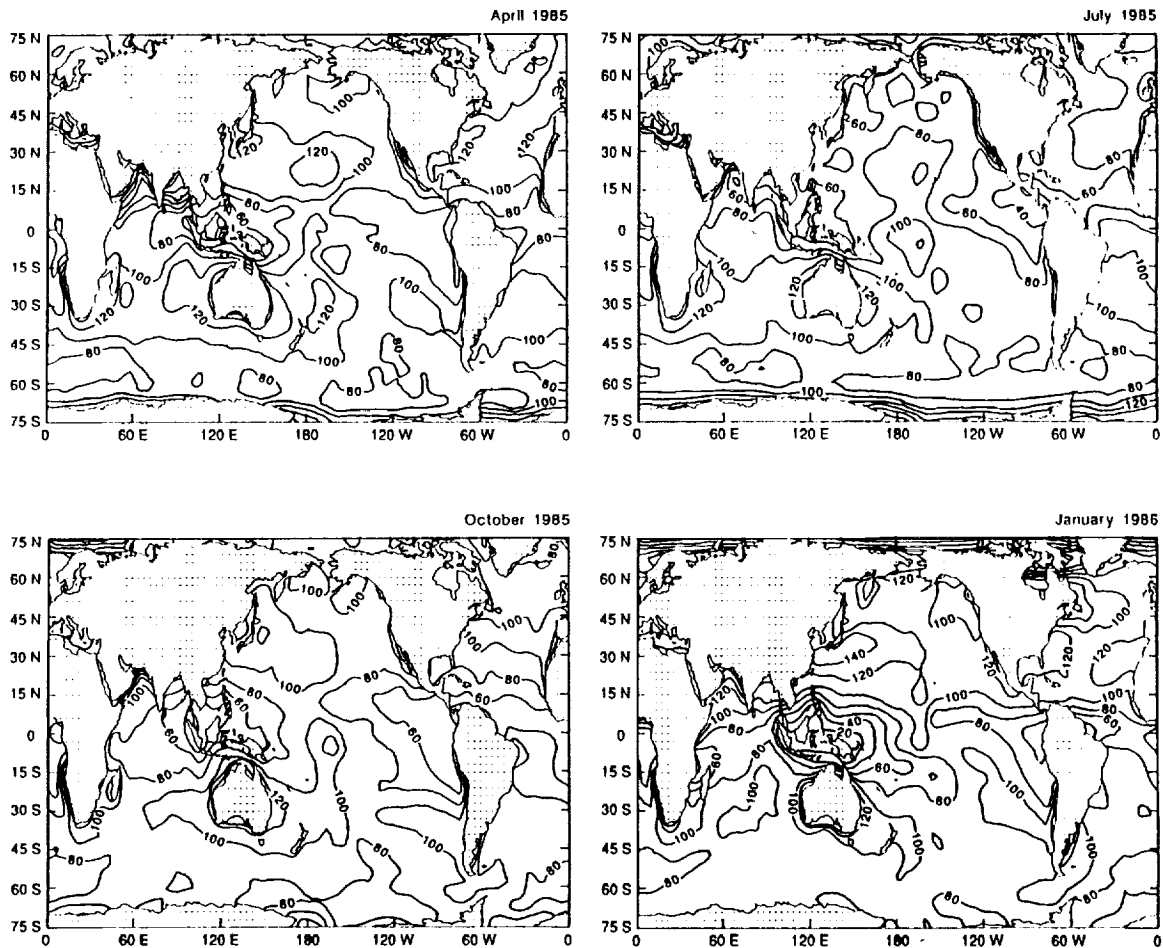## Clear Sky Net Upward Longwave Flux at the Surface

$$(W\,m^{-2})$$

Figure 7. Monthly mean clear sky net upward longwave radiation flux at the ocean surface for April, July, October 1985 and January 1986.

the stratus regime causes the net longwave flux to be reduced by 50-60 Wm^{-2} throughout the year. These maps again show features similar to those obtained by Wu and Cheng (1989).

4. Discussion

Monthly mean longwave radiation fluxes at the surface for four months have been determined from currently available satellite data. Because of the diurnal variation of surface temperature over the continents, surface net longwave fluxes, which involve the surface temperatures, are presented only over the oceanic areas.

As mentioned above, this method avoids the use of an independent estimate of the frequency of occurrence of clouds or even cloud top heights in determining the surface longwave fluxes. Current

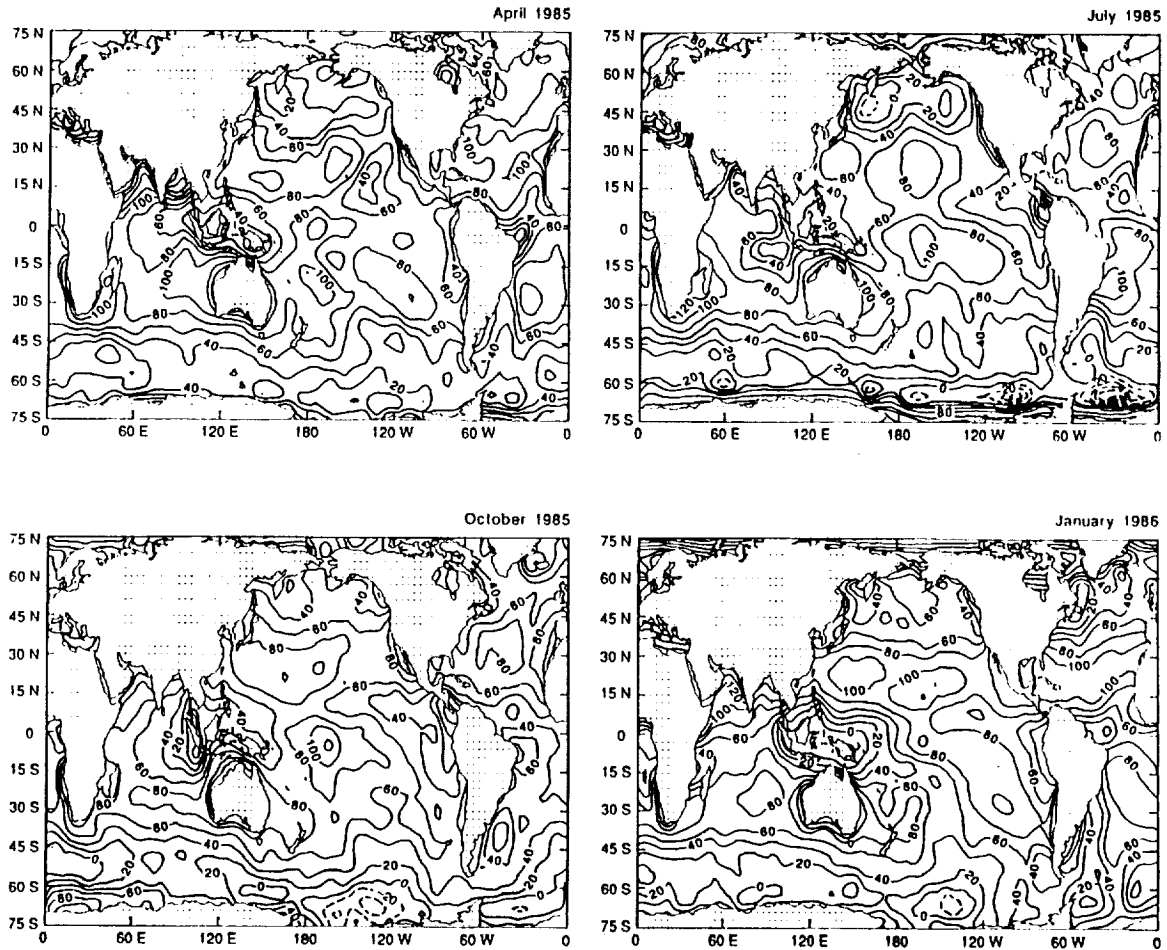Atmospheric Net Upward Longwave Flux at the Surface
$(W\ m^{-2})$

Figure 8.   Monthly mean atmospheric net upward longwave radiation flux at the ocean surface for April, July, October 1985 and January 1986.

methods of modeling the longwave radiation processes in the atmosphere require certain assumptions regarding the presence of clouds and their horizontal and vertical extent. Because of the complicated nature of cloud radiation and uncertainties in the observation of clouds, a large margin of error surely will be made in this procedure. The method here provides an alternative means of obtaining longwave radiative fluxes at the surface without the knowledge of cloud distribution. All meteorological parameters required in this method can be obtained from currently available satellite data sets. The ISCCP data and U.S. Standard Atmosphere (COESA 1976) provide the profiles of temperature, water vapor mixing ratio and ozone as well as sea surface temperatures. The distributions of the longwave CRF at the top of the atmosphere are retrieved from ERBE data which is currently being completed for several years of measurements.

The weakest link in this procedure is the use of simulated CRF ratios that relate the CRF at the top and surface. Errors in the cloud generation scheme of the model used will affect the ratio and hence, the final product. It is also not feasible to verify these ratios observationally on a global scale, although it would be useful to verify the model result in some specific regions where simultaneous observations at the top of the atmosphere and the surface are available over an extended period of time. However, most of the results in this study are generally consistent with currently known meteorological knowledge and explainable on the basis of previous theoretical and observational work and we feel that the field of mean surface longwave radiation fluxes produced here are useful.

References

Ardanuy, P.E., L.L. Stowe, A. Gruber, M. Weiss and S.L. Craig, 1989: Longwave cloud radiative forcing as determined from Nimbus-7 observations. *J. Climate*, 2, 766-799.

Breon, F.-M., R. Frouin and C. Gautier, 1991: Downward longwave irradiance at the ocean surface: an assessment of in situ measurements and parameterizations. *J. Appl. Meteor.*, 30, 17-31.

Charlock, T.P., and V. Ramanathan, 1985: The albedo field and cloud radiative forcing produced by a general circulation model with internally generated cloud optics. *J. Atmos. Sci.*, 42, 1408-1429.

Chou, M.D., 1985: Surface radiation in the tropical pacific. *J. Climate Appl. Meteor.*, 24, 83-92.

COESA, U.S. Standard Atmosphere, 1976: U.S. Government Printing Office, Washington D. C.. Darnell, W.L., S.K. Gupta and W.F. Staylor, 1983: Downward longwave radiation at the surface from satellite measurement. *J. Climate Appl. Meteor.* 22, 1956-1960.

Darnell, W.L., S.K. Gupta and W.F. Staylor, 1986: Downward longwave surface radiation from sun-synchronous satellite data: Validation of methodology. *J. Climate Appl. Meteor.* 25, 1012-1021.

Frouin, R., C. Gautier and J. Morcrette, 1988: Downward longwave irradiance at the ocean surface from satellite data: Methodology and in situ validation. *J. Geophys. Res.*, 93, 597-619.

Gautier, C., G. Diak and S. Masse, 1980: A simple physical model to estimate incident solar radiation at the surface from GOES satellite data. *J. Appl. Meteor.*, 19, 1005-1012.

Gupta, S.K., 1989: A parameterization for longwave surface radiation from sun-synchronous satellite data. *J. Climate*, 2, 305-320.

Harshvardhan, D.A. Randall, T.G. Corsetti and D.A. Dazlich, 1989: Earth radiation budget and cloudiness simulations with a general circulation model. *J. Atmos. Sci.*, **46**, 1922-1942.

Harshvardhan, D.A. Randall, and D.A. Dazlich, 1990: Relationship between the longwave cloud radiative forcing at the surface and the top of the atmosphere. *J. Climate*, **3**, 1435-1443.

Justus, C.G., M.V. Paris and J.D. Tarpley, 1986: Satellite-measured insolation in the United States, Mexico, and South America. *Remote Sens. Envir.*, **20**, 57-83.

Pinker, R.T. and J.A. Ewing, 1985: Modeling surface solar radiation: Model formulation and validation. *J. Climate Appl. Meteor.*, **24**, 389-401.

Ramanathan, V., 1986: Scientific use of surface radiation budget data for climate studies. *Surface Radiation Budget for Climate Studies.* J.T. Suttles and G. Ohring, Eds., NASA reference publication 1169, 132pp.

Ramanathan, V., 1987: The role of Earth radiation budget studies in climate and general circulation research. *J. Geophys. Res.*, **92**, 4075-4095.

Randall, D.A., Harshvardhan, D.A. Dazlich and T.G. Corsetti, 1989: Interactions among radiation, convection, and large-scale dynamics in a general circulation model. *J. Atmos. Sci.*, **46**, 1943-1970.

Randall, D.A., Harshvardhan, and D.A. Dazlich, 1991: Diurnal variability of the hydrologic cycle in a general circulation model. *J. Atmos. Sci.*, **48**, 40-62.

Raschke, E., and H.J. Preuss, 1979: The determination of solar radiation budget at the Earth's surface from satellite measurements. *Meteor. Rundsch.*, **32**, 18-28.

Reynolds, R. W., 1988: A real-time global sea surface temperature analysis. *J. Climate*, **1**, 75-86.

Schiffer, R.A., and W.B. Rossow, 1983: The International Satellite Cloud Climatology Project (ISCCP): The first project of the world climate research programme. *Bull Amer. Meteor. Soc.*, **64**, 779-784.

Schmetz, P., J. Schmetz and E. Raschke, 1986: Estimation of daytime downward longwave radiation at the surface from satellite and grid point data. *Theor. Appl. Climatol.*, **37**, 136-149.

Tarpley, J.D., 1979: Estimating incident solar radiation at the surface from geostationary satellite data. *J. Appl. Meteor.*, **18**, 1172-1181.

WCP-92, 1984: World Climate Research Programme, WMO, GENEVA, Switzerland.

Weare, B.C., 1989: Relationships between net radiation at the surface and the top of the atmosphere derived from a general circulation model. *J. Climate*, **2**, 193-197.

Wu, M.-L.C., and C.-P. Cheng, 1989: Surface downward flux computed by using geophysical parameters derived from HIRS 2/MSU soundings. *Theor. Appl. Climatol.*, **40**, 37-51.